BJ www.biochemj.org

Biochem. J. (2011) **439**, 265–275 (Printed in Great Britain) doi:10.1042/BJ20110150

online data

Laforin, a dual-specificity phosphatase involved in Lafora disease, is phosphorylated at Ser[25] by AMP-activated protein kinase

Carlos ROMÁ-MATEO*, Maria del Carmen SOLAZ-FUSTER*, José Vicente GIMENO-ALCAÑIZ*, Vikas V. DUKHANDE†, Jordi DONDERIS*, Carolyn A. WORBY‡, Alberto MARINA*, Olga CRIADO§, Antonius KOLLER‖, Santiago RODRIGUEZ DE CORDOBA§, Matthew S. GENTRY†[1,2] and Pascual SANZ*[1,2]

*Instituto de Biomedicina de Valencia, CSIC and Centro de Investigación Biomédica en Red de Enfermedades Raras (CIBERER), Jaime Roig 11, 46010 Valencia, Spain, †Department of Molecular and Cellular Biochemistry and Center for Structural Biology, University of Kentucky, Lexington, KY 40536-0509, U.S.A., ‡Departments of Pharmacology, Cellular and Molecular Medicine, and Chemistry and Biochemistry, University of California San Diego, La Jolla, CA 92093-0721, U.S.A., §Centro de Investigaciones Biológicas, CSIC and Centro de Investigación Biomédica en Red de Enfermedades Raras (CIBERER), Ramiro de Maeztu 9, 28040 Madrid, Spain, and ‖Proteomics Center, SUNY-Stony Brook, School of Medicine, Stony Brook, NY 11794-8691, U.S.A.

Lafora progressive myoclonus epilepsy [LD (Lafora disease)] is a fatal autosomal recessive neurodegenerative disorder caused by loss-of-function mutations in either the *EPM2A* gene, encoding the dual-specificity phosphatase laforin, or the *EPM2B* gene, encoding the E3-ubiquitin ligase malin. Previously, we and others showed that laforin and malin form a functional complex that regulates multiple aspects of glycogen metabolism, and that the interaction between laforin and malin is enhanced by conditions activating AMPK (AMP-activated protein kinase). In the present study, we demonstrate that laforin is a phosphoprotein, as indicated by two-dimensional electrophoresis, and we identify Ser[25] as the residue involved in this modification. We also show that Ser[25] is phosphorylated both *in vitro* and *in vivo* by AMPK. Lastly, we demonstrate that this residue plays a critical role for both the phosphatase activity and the ability of laforin to interact with itself and with previously established binding partners. The results of the present study suggest that phosphorylation of laforin-Ser[25] by AMPK provides a mechanism to modulate the interaction between laforin and malin. Regulation of this complex is necessary to maintain normal glycogen metabolism. Importantly, Ser[25] is mutated in some LD patients (S25P), and our results begin to elucidate the mechanism of disease in these patients.

Key words: alanine scanning mutagenesis, AMP-activated protein kinase (AMPK), glucan-phosphatase, laforin, phosphorylation, protein–protein interaction.

INTRODUCTION

Lafora progressive myoclonus epilepsy [LD (Lafora disease), OMIM 254780] is a fatal autosomal recessive neurodegenerative disorder characterized by the presence of progressive neurological deterioration, myoclonus and epilepsy (for reviews, see [1,2]). LD initially manifests during adolescence with generalized tonic–clonic seizures, myoclonus, absences, drop attacks and visual hallucinations. As the disease proceeds, patients enter into a vegetative state and eventually die, usually within the first decade from onset of the first symptoms [1,3]. Mutations causing LD have been identified in two genes, *EPM2A* [4,5] and *EPM2B* (*NHLRC1*) [6], and there is evidence for a third locus [7].

EPM2A encodes laforin, a dual-specificity phosphatase with a functional carbohydrate-binding domain at the N-terminus [8,9]. *EPM2B* encodes malin, an E3-ubiquitin ligase with a RING finger domain at the N-terminus and six NHL domains involved in protein–protein interactions in the C-terminal region [6,10,11]. A hallmark of LD is the accumulation of insoluble glucans (i.e. carbohydrates) called LBs (Lafora bodies) [12,13]. LBs form in the cytoplasm of cells from most tissues. LBs, like normal glycogen, are composed of glucose residues joined by α-1,4-glycosidic linkages with branches occurring via α-1,6-glycosidic linkages (reviewed in [2]). However, the branches are less frequent in LBs compared with glycogen, making LBs water-insoluble. It has been described previously that laforin directly interacts with malin, forming a laforin–malin complex, and that laforin recruits specific substrates to be ubiquitinated by malin [10,11,14]. Given the reoccurring theme of glycogen and carbohydrates in LD, it is not surprising that some substrates of the laforin–malin complex are integrally involved in regulating glycogen biosynthesis. The laforin–malin complex ubiquitinates MGS (muscle isoform of glycogen synthase) [15], GDE [glycogen debranching enzyme; also known as AGL (amylo-α-1,6-glucosidase)] [16], and the glycogen targeting subunit of PP1 (type 1 protein phosphatase) called R5/PTG (protein targeting to glycogen) [14,17]. Although multiple groups have corroborated these findings, there is dissent concerning whether they are *in vivo* substrates of the malin–laforin complex [18,19].

Despite these important genetic findings, the physiological roles of laforin and malin are only beginning to be understood, and it is still unclear which cellular processes, altered by the absence of these proteins, give rise to the devastating disorder of LD. More recently, an alternative function for laforin in glycogen homoeostasis has been described [20–22]. In this case, laforin acts as a phosphatase of glycogen and it has been proposed that

Abbreviations used: AGL, amylo-α-1, 6-glucosidase; AMPK, AMP-activated protein kinase; CA, constitutively active; CBD, carbohydrate-binding domain; CHO, Chinese-hamster ovary; 2DE, two-dimensional electrophoresis; DMEM, Dulbecco's modified Eagle's medium; DSPD, dual-specificity phosphatase domain; DTT, dithiothreitol; GDE, glycogen debranching enzyme; GFP, green fluorescent protein; GST, glutathione transferase; HA, haemagglutinin; HEK, human embryonic kidney; Hs-laforin, human laforin; i.d., internal diameter; IEF, isoelectric focusing; IPG, immobilized pH gradient; KD, kinase dead; KO, knockout; LB, Lafora body; LC, liquid chromatography; LD, Lafora disease; MEF, mouse embryonic fibroblast; MGS, muscle isoform of glycogen synthase; MS/MS, tandem MS; OMFP, 3-*O*-methyl fluorescein phosphate; PP1, type 1 protein phosphatase; R5/PTG, protein targeting to glycogen; SC, synthetic complete; VHR, vaccinia H1-related; WT, wild-type.

[1] These senior authors contributed equally to this work.

[2] Correspondence may be addressed to either of these authors (email matthew.gentry@uky.edu or sanz@ibv.csic.es).

this function might be necessary for the maintenance of normal cellular glycogen [20,22,23].

We have previously demonstrated that the activity of the laforin–malin complex is modulated by AMPK (AMP-activated protein kinase), but no modified residue was identified and the mechanism driving this modulation is currently unknown [14]. However, it is clear that activated AMPK increases the interaction between laforin and malin, and the increased interaction enhances the degradation of R5/PTG by the laforin–malin complex [14]. The degradation of R5/PTG inhibits the glycogenic activity of R5/PTG and down-regulates glycogen production. Cumulatively, these results highlight the importance of the laforin–malin complex in regulating glycogen biosynthesis, and these molecular events are consistent with the accumulation of the glycogen-like intracellular LBs. However, despite these findings, it is currently unclear whether the accumulation of LBs is the cause of the disease or is a secondary determinant of a primarily established metabolic alteration.

As mentioned above, laforin is a dual-specificity phosphatase and as such contains a DSPD (dual-specificity phosphatase domain) at the C-terminus. Accordingly, recombinant laforin is able to dephosphorylate *in vitro* artificial substrates such as *p*-nitrophenylphosphate and OMFP (3-*O*-methyl fluorescein phosphate; a more sensitive substrate of dual-specificity phosphatases) [24–26]. In addition to the capacity of laforin to dephosphorylate glycogen (see above), it has been suggested that laforin dephosphorylates proteinaceous substrates such as GSK3β (glycogen synthase kinase 3β) [27,28], although this is a controversial issue [20,21].

In the present paper, we show evidence that laforin is a phosphoprotein that is phosphorylated at Ser^{25} by AMPK. In addition, we demonstrate that this residue plays critical roles in laforin function, affecting phosphatase activity and the ability of laforin to interact with itself and with previously established binding partners. Since Ser^{25} is mutated in some LD patients (S25P), the results of the present study begin to elucidate the mechanism of disease in this population of patients.

EXPERIMENTAL

Cell models, culture conditions and genetic methods

Escherichia coli DH5α was used as the host strain for plasmid constructions. *E. coli* BL21 (RIL) was used for protein production. These strains were grown in Luria–Bertani [1 % peptone, 0.5 % yeast extract, 1 % NaCl (pH 7.5)] medium supplemented with 50 mg/l ampicillin. Yeast strains used in the present study were FY250 (*MAT*α *his3*Δ*200 leu2*Δ*1 trp1*Δ*63 ura3-52*) and CTY10-5d (*MAT*a *ade2 his3 leu2 trp1 gal4 gal80 URA3*::lexAop-lacZ; a gift from Dr R. Sternglanz, State University of New York, Stony Brook, NY, U.S.A.). Yeast transformation was carried out using the lithium acetate protocol [29]. Yeast cultures were grown in SC (synthetic complete) medium lacking the corresponding supplements to maintain selection for plasmids [30].

HEK (human embryonic kidney)-293 cells, CHO (Chinese-hamster ovary) cells, and control and double AMPKα1α2-KO (knockout) MEFs (mouse embryonic fibroblasts; kindly provided by Dr Benoit Viollet, Institut Cochin, Université Paris Descartes, Paris, France) were grown in DMEM (Dulbecco's modified Eagle's medium; Lonza) supplemented with 100 units/ml penicillin, 100 μg/ml streptomycin, 2 mM glutamine and 10 % inactivated FBS (fetal bovine serum; Gibco). Cells (1.5×10^6) were plated on to 60-mm-diameter culture dishes the day before transfection. Cells were transfected with 1 μg of each plasmid using Lipofectamine™ 2000 (Invitrogen). In [^{32}P]P_i labelling experiments, cells were grown to sub-confluency, the cells were transfected and 24 h later the cells were washed with phosphate-free DMEM. Then, cells were incubated in DMEM-free medium for 0.5 h, 0.25 mCi/ml [^{32}P]P_i and 10 μM MG132 were added, the cells were incubated for 5 h, and denatured immunoprecipitations were preformed as described previously [11].

Plasmids

Plasmids pEG202-laforin S25A, T45A, T83A, S98A, T111A, T133A, T136A, T142A, T143A, S158A, S168A, T177A, T187A, T194I, S202/3A, T213A, T216A, T233A, S237/T238A, S273/T274A, S326A, S327A and S330A, were obtained by site-directed mutagenesis using plasmid pEG202-laforin [14] as the template, the QuikChange® kit (Stratagene) and the corresponding mutagenic oligonucleotides. These mutagenic nucleotides contained the corresponding 21 nucleotides upstream of the codon to be mutated and the downstream 21 nucleotides (45 nucleotides in total), based on Hs-laforin (human laforin) cDNA. Nucleotides in the mutated codon were replaced by the appropriated nucleotides to code for alanine (only in the case of T194I, nucleotides were changed to code for isoleucine). Similarly we constructed plasmids pEG202-laforin S25D, S168D, T187D and T194D. In this case, nucleotides in the mutated codon were changed to code for aspartate. The sequences of all of these mutagenic oligonucleotides are available upon request. All mutants were sequenced to ensure that additional mutations were not introduced during the mutagenesis procedure. Plasmids pACT2-laforin WT (wild-type), S25A, S25D and T194I were obtained by digesting the corresponding pEG202-laforin plasmids with BamHI and SalI and cloning the corresponding fragment into pACT2, digested with the same set of restriction enzymes.

Plasmids pCMVmyc-laforin WT, S25A, S25D and T194I were obtained by digesting the corresponding pACT2-laforin plasmids with SfiI and BglII and subcloning the corresponding fragment into pCMVmyc (BD Biosciences), digested with the same set of restriction enzymes. Plasmids pWSGST-laforin WT, S25A and S25D were obtained by digesting the corresponding pEG202-laforin plasmids with BamHI/SalI and subcloning the fragments into the pWSGST vector [31].

Other plasmids used in the present study were: pACT2-malin, pACT2-R5/PTG and pACT2-AMPKα2 [14]. Plasmid pGEX4T1-VHR (VHR is vaccinia H1-related) was a gift from Dr Rafael Pulido (Centro de Investigacion Principe Felipe, Valencia, Spain). Plasmid pEGFP-N1 was from BD Biosciences. pEGB2 AMPKα1 WT, KD (kinase dead, AMPKα1 D157A) and CA (constitutively active, AMPKα1 residues 1–312) were gifts from Dr Reuben Shaw (Salk Institute, San Diego, CA, U.S.A.) [32].

Yeast two-hybrid analyses

The yeast strain CTY10.5d was co-transformed with combinations of pACT2-malin, pACT2-R5/PTG and pACT2-AMPKα2 and different pEG202-laforin mutant plasmids. Transformants were grown in selective SC medium (4 % glucose) and shifted to low-glucose conditions (0.05 % glucose) for 3 h when indicated. Then, β-galactosidase activity was assayed in permeabilized cells and expressed in Miller Units, as described in [33].

Expression of recombinant proteins

E. coli transformants harbouring the pGEX4T1-VHR plasmid were grown in 500 ml of Luria–Bertani medium/ampicillin. Transformants were grown at 37 °C until the attenuance at 600 nm reached a value of approximately 0.3. IPTG (isopropyl

β-D-thiogalactopyranoside) was then added to a final concentration of 0.1 mM, and cultures were maintained overnight at 25 °C. Cells were harvested and resuspended in 20 ml of sonication buffer [50 mM Hepes/NaOH (pH 7.0), 150 mM NaCl, 10 % glycerol, 0.1 % Triton X-100, 2 mM DTT (dithiothreitol), 2 mM PMSF and Complete™ protease inhibitor cocktail (Roche)]. Cells were disrupted by sonication and the fusion proteins were purified by passing the extracts through columns containing a 1 ml bed volume of glutathione–Sepharose (GE Healthcare). GST (glutathione transferase)-fusion proteins were eluted from the column with 50 mM glutathione. Samples were stored at − 80 °C.

FY250 yeast cells were transformed with plasmids pWSGST-laforin WT, S25A and S25D. Yeast extracts were prepared as described in [34]. Extraction buffer was 50 mM Tris/HCl (pH 7.5), 150 mM NaCl, 0.1 % Triton X-100, 1 mM DTT and 10 % glycerol, and contained 2 mM PMSF and Complete™ protease inhibitor cocktail (Roche). GST-fusion proteins were purified and eluted as described above.

Immunodetection

HEK-293 cells were transfected with the corresponding plasmids. At 24 h after transfection, cells were scraped on ice in lysis buffer [10 mM Tris/HCl (pH 8), 150 mM NaCl, 15 mM EDTA, 0.6 M sucrose, 0.5 % Nonidet P40, Complete™ protease inhibitor cocktail (Roche), 1 mM PMSF, 50 mM NaF and 5 mM $Na_2P_2O_7$]. Cells were lysed by repeated passage through a 25-gauge needle. Total protein (25 μg) from the soluble fraction of cell lysates were analysed by SDS/PAGE and Western blotting using appropriate antibodies: anti-Myc, anti-tubulin (Sigma) and anti-GFP (green fluorescent protein; Immunokontact). Yeast extracts were prepared as described previously [34]; samples (15 μg) were separated by SDS/PAGE and analysed by Western blotting using the corresponding anti-LexA (Santa Cruz Biotechnology), anti-HA (haemagglutinin; Sigma) and anti-GST (GE Healthcare) antibodies.

Non-denaturing gel electrophoresis

Cell extracts were freshly prepared in SDS- and DTT-free loading buffer (125 mM Tris/HCl and 20 % glycerol), samples were not heated, and then were analysed by SDS/PAGE and Western blotting.

2DE (two-dimensional electrophoresis)

Mammalian HEK-293 cells were transfected with pCMVmyc-laforin (WT, S25D and T194I) plasmids and, 24 h after transfection, extracts were prepared in urea lysis buffer (9.7 M urea, 4 % CHAPS and 20 mM DTT). Myc–laforin derivatives were analysed by 2DE using an IPGphor (Amersham Biosciences) instrument. For the first dimension [IEF (isoelectric focusing)], 50 μg of total protein [in 100 μl of 9.7 M urea, 4 % CHAPS, 20 mM DTT and 0.5 % IPG (immobilized pH gradient) buffer] were loaded on to a 7 cm IPG strip (pH range 4–7) using the following focusing conditions: 500 V for 30 min, 1000 V for 30 min and 5000 V for 80 min. Electrophoretic separation (second dimension) was performed using SDS/PAGE. When indicated, extracts were also prepared in λ-phosphatase buffer containing 2 mM $MnCl_2$. The crude extract (50 μg) was treated at 30 °C for 30 min with 50 units of λ-phosphatase (New England Biolabs). Reactions were stopped by adding 2 vols of urea lysis buffer and were analysed by 2DE as described above. The same protocol was used to analyse MEFs transfected with pCMVmyc-laforin.

In vitro kinase assays

Kinase assays were performed with 5.0 ng of recombinant AMPK (Sigma) incubated with 100 ng of recombinant non-tagged Hs-laforin (Hs-laforin-NT) in kinase buffer [25 mM Mops (pH 7.2), 12.5 mM glycerol, 25 mM $MgCl_2$, 5 mM EDTA, 2 mM EGTA and 0.25 mM DTT] along with 0.5 mM AMP and 1 μCi of [γ-^{32}P]ATP (PerkinElmer). After 15 min at 30 °C, SDS/PAGE buffer was added to each sample at 4 °C to stop the reaction. Samples were separated by SDS/PAGE, followed by transfer on to PVDF and autoradiography.

Identification of phosphorylation sites

In vitro kinase assays were performed as described above in the absence of [γ-^{32}P]ATP. After purification of Hs-laforin by affinity chromatography, SDS/PAGE and Coomassie Blue staining, bands corresponding to Hs-laforin were excized from the gel. The gel slices were reduced with DTT and alkylated with iodoacetamide. Following in-gel trypsin and chymotrypsin digestion, the peptides were analysed by automated microcapillary LC-MS/MS (liquid chromatography-tandem MS). Fused-silica capillaries [100 μm i.d. (internal diameter)] were pulled using a P-2000 CO_2 laser puller (Sutter Instruments) to a 5 μm i.d. tip and packed with 10 cm of 5 μm Magic C_{18} material (Agilent) using a pressure bomb. This column was then placed in-line with a Dionex 3000 HPLC equipped with an autosampler. The column was equilibrated in buffer A (2 % acetonitrile and 0.1 % formic acid), and the peptide mixture was loaded on to the column using the autosampler. The HPLC separation at a flow rate of 300 nl/min was provided by a gradient between buffer A and buffer B (98 % acetonitrile, 0.1 % formic acid). The HPLC gradient was held constant at 100 % buffer A for 5 min after peptide loading followed by a 30 min gradient from 5 % buffer B to 40 % buffer B. Then, the gradient was switched from 40 % to 80 % buffer B over 5 min and held constant for 3 min. Finally, the gradient was changed from 80 % buffer B to 100 % buffer A over 1 min, and then held constant at 100 % buffer A for a further 15 min. The application of a 1.8 kV distal voltage electrosprayed the eluted peptides directly into a Thermo LTQ ion-trap mass spectrometer equipped with a custom nanoLC electrospray ionization source. Full masses (MS) spectra were recorded on the peptides over a 400–2000 *m*/*z* range, followed by five tandem mass (MS/MS) events sequentially generated in a data-dependent manner on the first, second, third, fourth and fifth most intense ions selected from the full MS spectrum (at 35 % collision energy). Mass spectrometer scan functions and HPLC solvent gradients were controlled by the Xcalibur data system (ThermoFinnigan). MS/MS spectra were extracted from the RAW file with ReAdW.exe (http://sourceforge.net/projects/sashimi). The resulting mzXML file contains all of the data for all MS/MS spectra and can be read by the subsequent analysis software. The MS/MS data were searched with InsPecT [35] against a database containing laforin in addition to an *E. coli* database plus common contaminants, with modifications: + 16 on methionine, + 57 on cysteine, and + 80 on serine, threonine and tyrosine. Only peptides with at least a *P* value of 0.01 were analysed further. Phosphorylated peptides were manually verified.

Carbohydrate-binding assay

Crude extracts from yeast cell cultures (400 ml) expressing GST–laforin (WT, S25A and S25D) were obtained as described above. Extracts (5 ml) were passed through columns containing a 150 μl bed volume of amylose–Sepharose (GE Healthcare). Flow-through was collected and columns were washed twice with

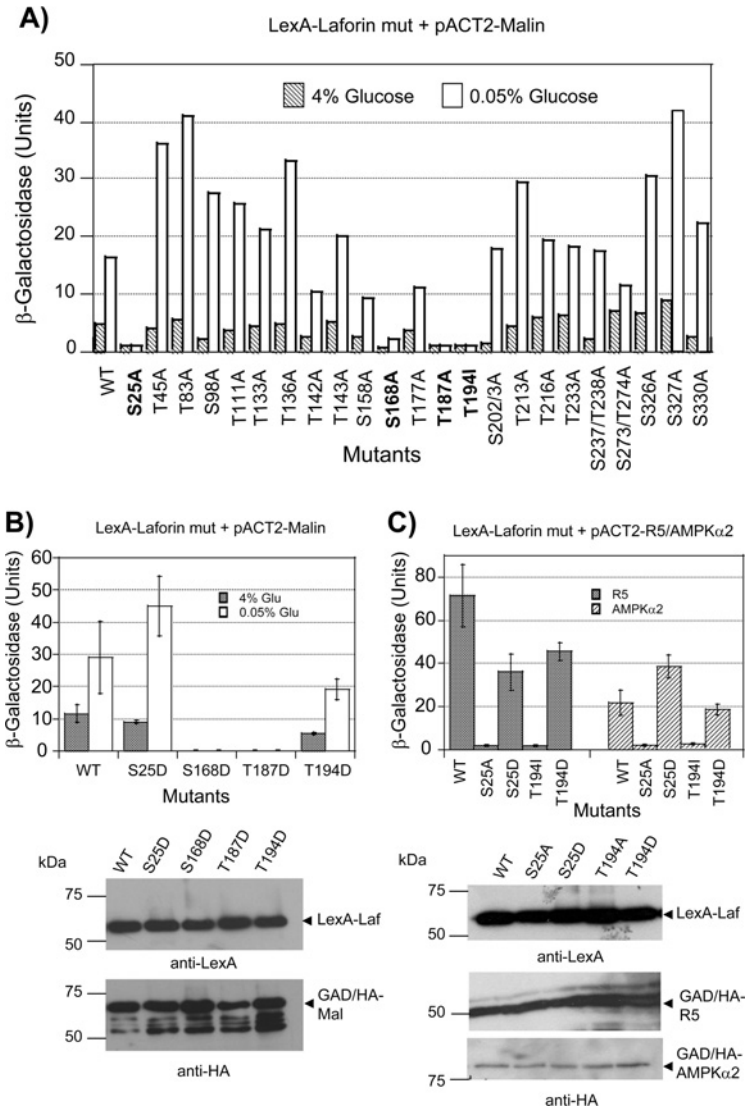

Figure 1 Alanine scanning mutagenesis of laforin and its effect on the interaction with malin

(**A**) pEG202-laforin plasmids containing the described mutations were introduced into CTY10-5d yeast strain in combination with plasmid pACT2-malin. Transformants were grown in 4 % glucose-containing medium until they reach exponential phase. Then, an aliquot of the cultures was shifted to low-glucose conditions (0.05 % glucose) for 3 h. Cells from both growth conditions were used to determine the β-galactosidase activity, as an indication of two-hybrid interaction (see the Experimental section). Results are the mean values from four to six different transformants, with an S.D. of less than 15 % in each case. (**B**) The two-hybrid interaction between the indicated plasmids was measured as described in (**A**); error bars indicate S.D. Yeast crude extracts (15 μg) from the different transformants were analysed by Western blotting using anti-LexA and anti-HA antibodies. Molecular mass standards are on the left-hand side. (**C**) The two-hybrid interaction between the corresponding protein fusions was measured as described above in cells growing in 4 % glucose; error bars indicate S.D. Yeast crude extracts (15 μg) from the different transformants were analysed by Western blotting using anti-LexA and anti-HA antibodies. Molecular mass standards are on the left-hand side.

5 ml of extraction buffer, collecting the second wash volume. Bound proteins were eluted with 50 μl of SDS/PAGE sample buffer. Collected samples (30 μl) were analysed by SDS/PAGE and Western blotting using anti-GST antibodies (GE Healthcare).

Phosphatase activity

In vitro phosphatase assays were performed using 4 μg of GST-fusion proteins diluted in phosphatase buffer (0.1 M Tris-HCl, 40 mM NaCl and 10 mM DTT), in the presence of 0.5 mM OMFP. Reactions were carried out at 37 °C in a final volume of 200 μl in 96-well ELISA plates. Phosphatase activity was measured for 3 h as absorbance at 490 nm. One unit of phosphatase activity is defined as one unit of change in the absorbance at 490 nm per min of assay.

Molecular modelling

HHpred search [36] and InterPro domain scan [37] were used to determine the best available template for modelling the CBD (carbohydrate-binding domain) and DSPD of laforin. The top three hits from each were aligned with the CBD of laforin using PROfile Multiple Alignment with predicted Local Structure 3D (PROMALS) [38]. A homology model for the CBD of laforin was generated using the ESyPred3D server [39] with the PDB code 1CYG (*Geobacillus stearothermophilus* cyclodextrin glycosyltransferase; 29 % identity) as the template. Similarly, the PDB code 1WRM (*Homo sapiens* DUSP22 phosphatase; 13.2 % identity) was used to generate a homology model for the laforin DSPD. Cyclodextrin moieties were docked after superimposition of the laforin CBD structural model with the *Aspergillus niger*

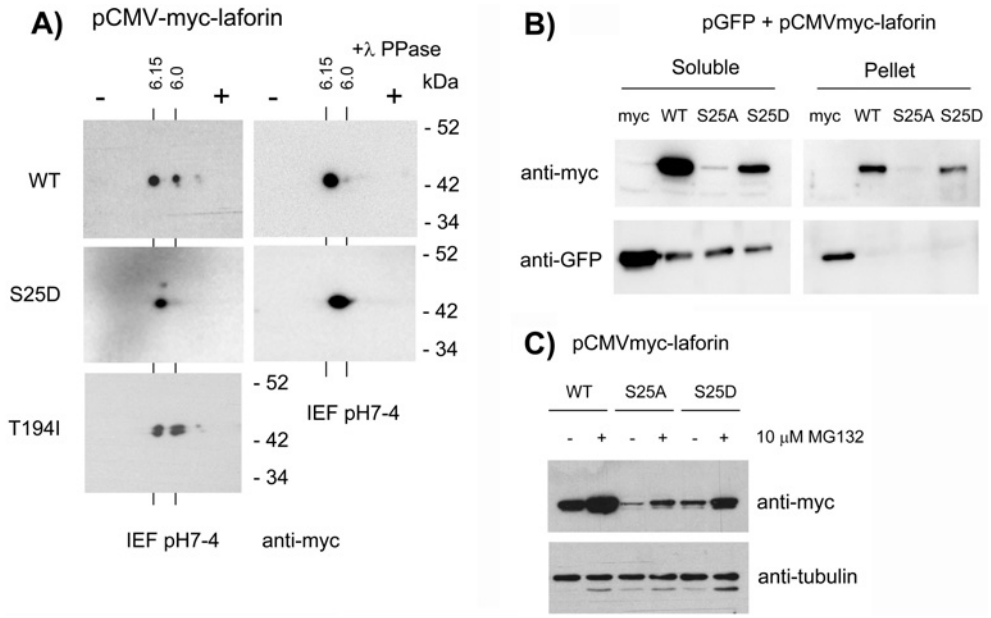

Figure 2 Laforin is phosphorylated at residue Ser[25]

(**A**) Cell extracts from HEK-293 cells transfected with plasmids pCMVmyc-laforin (WT, S25D and T194I) were analysed by 2DE and Western blotting using anti-Myc monoclonal antibodies. Cell extracts were also treated with λ-phosphatase as described in the Experimental section. The calculated pI for each spot is indicated. Molecular mass standards are indicated on the right-hand side. (**B**) Cell extracts from HEK-293 cells co-transfected with plasmids pCMVmyc-laforin (WT, S25A and S25D) and pEGFP-N1 (expressing GFP) were prepared for immunodetection as described in the Experimental section. In this case, the lysis buffer contained 0.5 % Triton X-100 instead of 0.5 % Nonidet P40. Extracts were centrifuged at 15 000 ***g*** for 10 min at 4 °C to separate soluble fractions from pellet fractions. These fractions were treated with SDS/PAGE sample buffer and analysed by Western blotting using anti-Myc and anti-GFP antibodies. (**C**) HEK-293 cells co-transfected with plasmids pCMVmyc-laforin (WT, S25A and S25D) were treated or not with 10 μM MG132 (a proteasome inhibitor) for 8 h. Then, crude extracts were obtained and analysed by Western blotting using anti-Myc and anti-tubulin (loading control) antibodies.

glucoamylase CBD structure (PDB code 1AC0). Images were generated with PyMOL (http://www.pymol.org).

Statistical analyses

Values are given as means ± S.D. for at least three independent experiments. When indicated, differences between groups were analysed by two-tailed Student's t tests. The significance has been considered at $^{*}P < 0.05$ and $^{**}P < 0.01$, as indicated in each case.

RESULTS

Mutation of serine/threonine residues to alanine influences the interaction of laforin with malin and with other established binding partners

We and others have described that laforin interacts physically with malin [10,11,14]. We have also previously described that the interaction between laforin and malin is enhanced by conditions that activate AMPK (a sensor of energy status), such as low-glucose conditions. In addition, we have demonstrated that laforin, but not malin, directly interacted with different subunits of the AMPK complex [14]. To test whether phosphorylation of laforin is responsible for the enhanced interaction between laforin and malin, we substituted each of the 26 serine/threonine residues present in laforin with alanine residues and analysed, by yeast two-hybrid analysis, the strength of the laforin–malin interaction. As reported previously, the two-hybrid interaction between WT laforin and malin increased under low-glucose conditions (Figure 1A), possibly because of the action of activated endogenous SNF1 (sucrose non-fermenting 1) complex (the yeast AMPK orthologue) [14]. We then analysed the interaction between mutated laforin and malin and observed that some serine/threonine to alanine replacements did not greatly affect the glucose-regulated interaction between laforin and malin, whereas others improved the interaction between these two proteins under low-glucose conditions (i.e. T45A, T83A, T136A, S327A, etc.). However, only four mutations abolished the interaction between laforin and malin, in both high- and low-glucose conditions, namely S25A, S168A, T187A and T194I (in the latter case, the threonine residue was replaced by isoleucine to mimic a mutation recovered from LD patients [40]). Western blot analyses confirmed that all of the mutated forms were expressed at similar levels (results not shown).

We reasoned that if the phosphorylation of one of these residues was responsible for the enhanced interaction between laforin and malin under low-glucose conditions, then substitution of this residue to the phosphomimetic residue aspartate should recover the interaction between laforin and malin. Thus we constructed the corresponding serine/threonine to aspartate mutants and observed that, in the case of the S168D and T187D mutants, the interaction with malin was still impaired, suggesting that these two residues may play important roles in the conformation of the protein and changes to either alanine or aspartate could severely affect the overall structure of the protein. Alternatively, in the case of S25D and T194D, the interaction with malin was recovered, although this recovery was lower in the T194I mutant (Figure 1B; Western blot analyses confirmed that the mutated forms were expressed at similar levels as WT). In the case of the S25D mutant, the interaction with malin under low-glucose conditions was greater than in WT, suggesting that a negative charge on this residue allowed a better regulation of the interaction between laforin and malin by glucose.

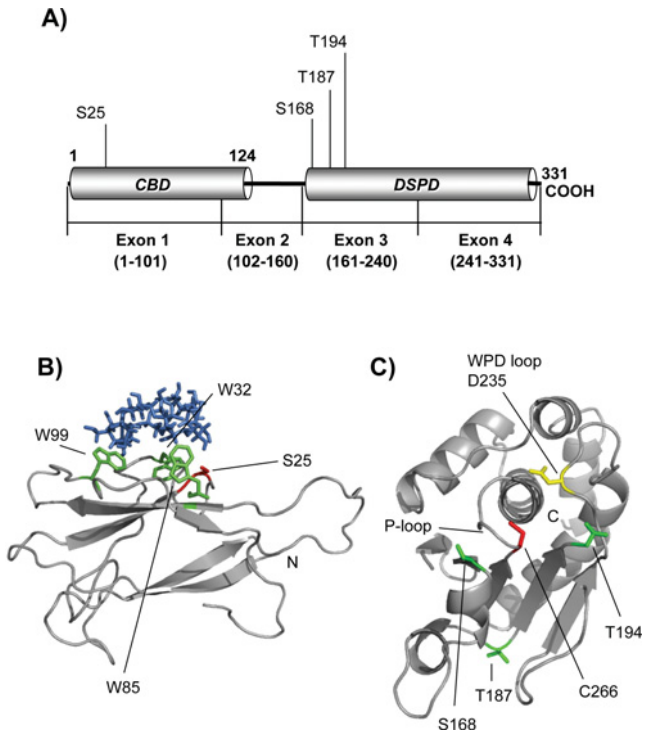

Figure 3 Structure models of the laforin CBD and DSPD

(**A**) Diagram of the position of the CBD and DSPD in the primary structure of Hs-laforin. The positions of residues described in the present study are also indicated. (**B**) The laforin CBD (residues 1–116) was *in silico* modelled, as described in the Experimental section, using the crystal structure of *G. stearothermophilus* cyclodextrin glycosyltransferase (PDB code 1CYG) as a template. The positions of the tryptophan residues involved in carbohydrate binding (Trp^{32}, Trp^{85} and Trp^{99}) are indicated in green and the position of residue Ser^{25} is marked in red. β-Cyclodextrin is coloured in blue. The N-terminus is also indicated. (**C**) The laforin DSPD (residues 157–326) was *in silico* modelled, as described in the Experimental section, using the crystal structure of human DUSP22 (PDB code 1WRM) as a template. The position of the characteristic P-loop, containing the catalytic Cys^{266} residue (in red), and the WPD-loop, containing the conserved Asp^{235} (in yellow), is indicated. The positions of other residues described in the present study (Ser^{168}, Thr^{187} and Thr^{194}; in green) and the C-terminus are also indicated.

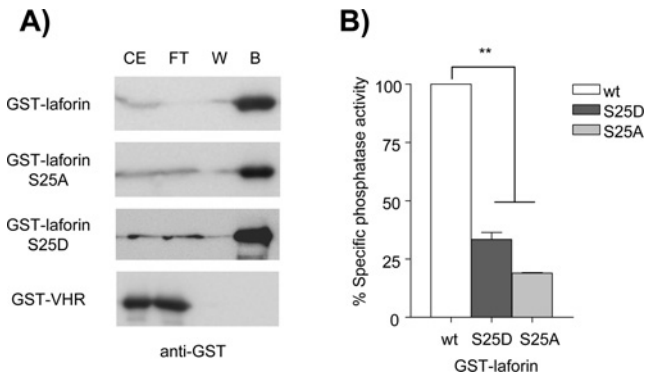

Figure 4 Effect of laforin-S25A/D mutations on carbohydrate-binding capacity and phosphatase activity

(**A**) Laforin-S25A and S25D mutations do not affect the carbohydrate-binding capacity of laforin. Yeast crude extracts (CE) containing GST–laforin (WT, S25A and S25D) and GST–VHR fusion proteins were passed through columns containing amylose–Sepharose. Flow-through (FT) was collected and columns were washed twice with 5 ml of extraction buffer, collecting the last wash (W). Bound proteins (B) were eluted with 50 μl of SDS/PAGE sample buffer. Collected samples were analysed by SDS/PAGE and Western blotting using anti-GST antibodies. A similar volume (30 μl) of CE, FT and the corresponding W was analysed. (**B**) Effect of S25A and S25D mutations on phosphatase activity of laforin. Phosphatase activity was measured on GST–laforin WT, S25A and S25D proteins purified from yeast. Phosphatase activity was referred to the activity found in the corresponding WT laforin. Statistical significance was considered at $^{**}P < 0.01$ ($n = 3$).

In addition to interacting with malin, we have also described that laforin interacts with the PP1 regulatory subunit R5/PTG and with subunits of the AMPK complex [14]. Therefore we investigated whether mutations in Ser^{25} and Thr^{194} affected the interaction with these partners. We observed that the S25A and T194I mutants did not interact with either R5/PTG or AMPKα2, whereas the S25D and T194D forms allowed the interaction with these components (Figure 1C; Western blot analyses confirmed that the mutated forms were expressed at similar levels as WT).

Laforin is a phosphoprotein and is phosphorylated on Ser^{25}

The results described above indicated that the replacement of serine/threonine residues (Ser^{25} and Thr^{194}) by non-phosphorylatable residues (alanine and isoleucine respectively) prevented the interaction of laforin with different binding partners. These results suggested that either the presence of a polar amino acid (serine/threonine) or the phosphorylation of these residues could be essential for the interaction of laforin with its corresponding partners. To discern between the two, we expressed the mutated forms in mammalian cells (HEK-293 cells) and analysed their *in vivo* phosphorylation status by 2DE. As shown in Figure 2(A) (top left-hand panel), WT laforin migrates as two major species on 2DE, indicative of phosphoprotein species. Furthermore, treatment of the sample with λ-phosphatase eliminated the spot that moved faster towards the positive pole (right-hand spot), suggesting that this form is due to phosphorylation (Figure 2A, top right-hand panel). The isoelectric point of the left-hand spot was in agreement with the calculated pI for the Myc–laforin fusion protein (pI of 6.15) and the isoelectric point of the right-hand spot (pI of 6.00) was compatible with the acquisition of one phosphate group.

We attempted to analyse the phosphorylation pattern of a laforin-S25A mutant, but the steady-state levels of this protein were greatly diminished (Figure 2B). Co-transfection experiments using a plasmid expressing GFP under the same promoter as the laforin constructs indicated that the low levels of the laforin-S25A protein were not due to different transfection efficiencies, since similar levels of GFP were observed in cells co-transfected with laforin or laforin-S25A constructs. In addition, laforin-S25A was not in the pellet after a high-speed spin, indicating that it did not form insoluble aggregates (Figure 2B). These results indicate that the stability of the laforin-S25A form could be greatly reduced, probably due to enhanced proteolytic turnover. In agreement with this proposal we observed an accumulation of laforin-S25A protein when the cells were treated with the proteasome inhibitor MG132 (Figure 2C). Therefore, although we cannot discard the possibility that the S25A mutation could affect the stability of the corresponding mRNA when expressed in mammalian cells, our results suggest that the laforin-S25A form is very unstable and gets rapidly degraded by the cellular proteolytic system. The reduced levels of laforin-S25A were only observed when the constructs were expressed in mammalian cells, but not when they were expressed in yeast (see Figure 1).

Since laforin-S25D was expressed in mammalian cells (although at lower levels than WT), we used this form in the 2DE experiments. We observed that laforin-S25D migrated as a single spot and treatment of the extracts with λ-phosphatase did not produce any shift in its mobility, indicating that this form was not phosphorylated *in vivo* (Figure 2A, middle panels). Owing to the negative charge of the new aspartate residue, this form migrated

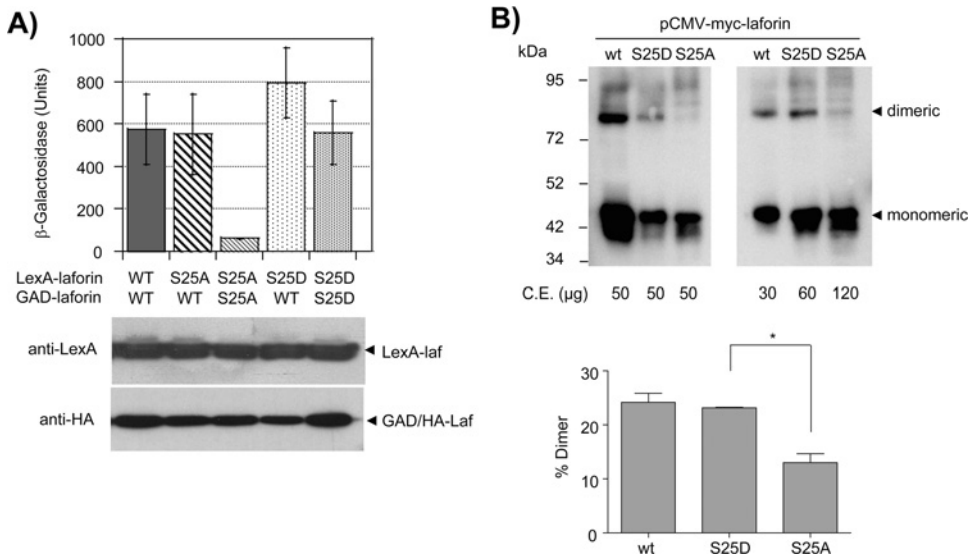

Figure 5 Effect of laforin-S25A/D mutations on dimerization capability

(**A**) CTY10-5d yeast cells transformed with the indicated plasmids were used to measure the two-hybrid interaction between the indicated proteins, as described in the legend to Figure 1. Results are the means ± S.D. for four to six different transformants. Yeast crude extracts (15 μg) from the different transformants were analysed by Western blotting using anti-LexA and anti-HA antibodies. (**B**) Crude extracts from CHO cells transfected with plasmid pCMVmyc-laforin (WT, S25D and S25A) were analysed by non-denaturing electrophoresis and Western blotting using anti-Myc monoclonal antibodies. Different amounts of the extracts were loaded as indicated. C.E., crude extracts. The molecular mass in kDa is indicated on the left-hand side. The lower panel shows the quantification of the proportion of dimers in cells expressing the different laforin forms. Values are means ± S.D. for three independent experiments ($^*P < 0.05$).

between pI 6.15 and 6.0. Conversely, laforin-T194I showed the presence of two major spots that migrated at similar isoelectric points as those that we observed for WT laforin (Figure 2A, bottom panel) (the observed doublet in each spot could be due to partial degradation of the sample).

Cumulatively, these results indicate that laforin is a phosphoprotein *in vivo* and that Ser[25] is the residue that is phosphorylated. The lack of interaction between laforin-S25A with malin, R5/PTG and AMPK is likely to be due to either the absence of Ser[25] phosphorylation or most likely to an altered conformation of the laforin-S25A mutant. In contrast, the decreased interaction of laforin-T194I with these proteins is likely to be due to a conformational change owing to the presence of a non-polar Ile[194] residue and not to a lack of phosphorylation of this mutant.

Mutation of Ser[25] to either alanine or aspartate maintains binding to carbohydrates but reduces phosphatase activity

Since no crystal structure of laforin is available yet and in order to map the position of the Ser[25] residue in the laforin molecule, we modelled the structure of the CBD of laforin (residues 1–116) (Figures 3A and 3B). We first searched the published CBD crystal structures to identify the best template for homology modelling. We identified the *G. stearothermophilus* cyclodextrin glycosyltransferase (PDB code 1CYG) as having the maximum identity with laforin (29 %) and generated a homology model using 1CYG as the template. The homology model suggested that the laforin CBD folds into the characteristic two β-sheets fold, each consisting of three to six antiparallel β-strands and with the N- and C-termini pointing towards opposite ends of the longest axis of the molecule (Figures 3A and 3B) [41]. Conserved aromatic residues involved in carbohydrate binding were readily observable in the laforin CBD structure: Trp[32], Trp[85] and Trp[99]. In the model, these residues form a compact, rigid and surface-exposed hydrophobic site containing inter-ring spacing appropriate for binding to α(1,4)-linked glucoses, as is the case for glycoamylase [41]. These results are similar to those reported previously when the laforin CBD was modelled based on the crystal structure of *Bacillus circulans* cyclodextrin glycosyltransferase (PDB code 2DIJ) [9]. In both cases, Ser[25] is located at the beginning of a hairpin loop, close to the carbohydrate-binding area (Figure 3B).

We also modelled the laforin DSPD (residues 157–326) by comparing it with that of the human DUSP22 phosphatase (PDB code 1WRM) [42] (Figure 3C). Again, this *in silico* approach suggested that the laforin DSPD folded into the characteristic fold consisting of four to five β-sheets surrounded by α-helices [43]. In this structure, the characteristic P-loop (phosphate-binding loop), containing the catalytic Cys[266] residue and the WPD-loop (TPD235 in laforin) with the conserved aspartate residue (Asp[235]) pointing towards the catalytic groove were clearly observed (Figure 3C). In this structure we were also able to map the position of Ser[168], Thr[187] and Thr[194], whose mutation to alanine (isoleucine in the case of Thr[194]) resulted in impairment of interaction of laforin with different binding partners (see above).

Ser[25] is a site mutated in some LD patients. Since it is close to the carbohydrate-binding area, we analysed whether modifications in this residue could affect carbohydrate binding. With this aim we expressed GST–laforin WT, S25A and S25D in yeast, as we were unable to produce the laforin-S25A mutant in bacteria. In addition, we expressed a human GST–VHR fusion protein as a control. VHR is a dual-specificity protein phosphatase that lacks a CBD [44]. As observed in Figure 4(A), GST–laforin WT, S25A and S25D were all able to bind to amylose–Sepharose. In contrast, GST–VHR did not bind the amylose–Sepharose, as expected. These results indicate that changing Ser[25] to a small non-polar (alanine) or to an acidic (aspartate) amino acid does not affect the capacity of laforin to interact with carbohydrates.

We next measured the *in vitro* phosphatase activity of the laforin mutants using OMFP as the substrate (Figure 4B). We

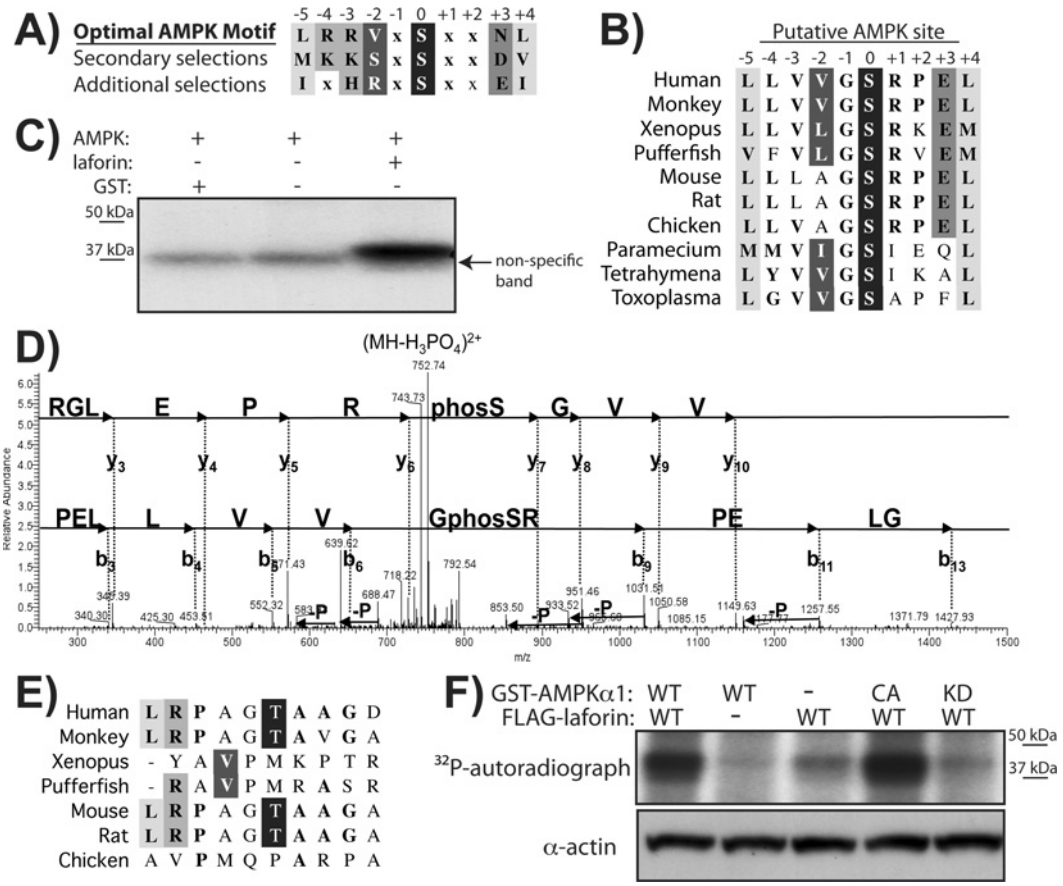

Figure 6 AMPK phosphorylates laforin at Ser[25]

(**A**) Optimal AMPK motifs [46]. (**B**) Evolutionary conservation of a putative AMPK site at Ser[25] of laforin. (**C**) *In vitro* phosphorylation of recombinant non-tagged laforin by recombinant AMPK. (**D**) MS/MS identification of the phosphorylation site Ser[25] in the laforin tryptic peptide PELLVVGSRPELGR. Individual fragment ions are labelled [*y*-ions, blue; *b*-ions, green; — P denotes the neutral loss of H_3PO_4 (— 98 Da)]. (**E**) Evolutionary conservation of Thr[45] of laforin. (**F**) HEK-293 cells were transfected with FLAG–laforin and AMPKα1 WT, KD and CA forms or empty vector, as indicated. Cells were incubated in [^{32}P]P_i and MG132 as described in the Experimental section. Laforin was immunoprecipitated, proteins were separated by SDS/PAGE, and the resulting gel was dried and exposed to film. Actin levels were used as a loading control of the amount of proteins in the crude extracts.

observed that both mutated laforins showed a dramatic decrease in phosphatase activity, which was more severe in the case of laforin-S25A (20 % with respect to WT). These results indicate that the replacement of Ser[25] by either a phosphomimetic aspartate residue or a non-polar residue (alanine) appears to impair the phosphatase activity of laforin.

Mutations in Ser[25] affect dimerization of laforin

It has been described in the literature that laforin forms dimers and that mutations in the CBD of laforin prevent the dimerization of the protein [45]. In order to determine whether dimerization is affected by the S25A/D mutants, we measured by two-hybrid analysis the capacity of the different forms to interact with each other. As shown in Figure 5(A), WT laforin strongly interacted with itself, in agreement with the reports on dimerization [45]. However, the laforin S25A mutant was unable to interact with itself, although it could form a stable interaction with WT laforin. Alternatively, laforin S25D was able to interact with itself and also with WT laforin. Western blot analyses confirmed that the mutated forms were expressed at similar levels as WT.

Next, we sought to extend our dimerization studies from yeast into mammalian cells. Since the expression of the S25A form in HEK-293 cells was very poor (see above), we tested different mammalian cell lines for their capacity to express the S25A mutants and found that CHO cells are able to express laforin S25A, although at lower levels than WT. Extracts from these cells were subjected to non-denaturing electrophoresis (in the absence of SDS and DTT) in order to detect the presence of dimeric forms of laforin. As shown in Figure 5(B), either by loading an equal amount of total protein (left-hand panel) or when we adjusted the amount of laforin in the lanes (right-hand panel), we observed the formation of dimeric forms in WT and S25D, but an impairment in the formation of these dimers in the S25A mutant (bottom panel shows the quantification of the proportion of dimers in the different laforin forms). These results confirmed our previous yeast two-hybrid data (Figure 5A) and clearly indicated that, in mammalian cells, dimerization of S25A mutant is prevented.

AMPK phosphorylates laforin at Ser[25]

With the identification of Ser[25] as the phosphorylation site, we then set out to determine the kinase that phosphorylates laforin. Given that AMPK and laforin interact with each other [14], we searched the primary sequence of laforin for putative AMPK consensus motifs. It was previously determined that AMPK has preferences at six positions surrounding the

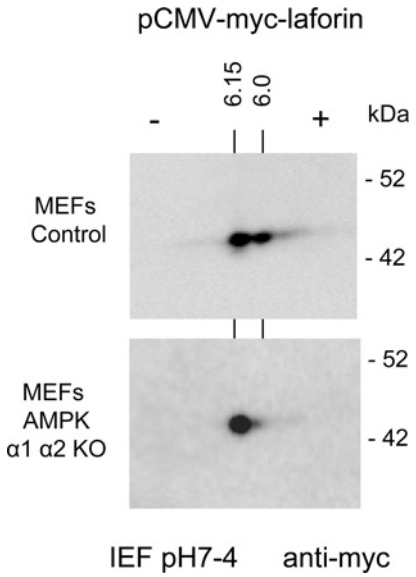

Figure 7 Laforin is not phosphorylated in the absence of AMPK

MEFs from control and double AMPKα1α2-KO mice were transfected with plasmid pCMVmyc-laforin. Cell extracts were analysed by 2DE and Western blotting using anti-Myc monoclonal antibodies, as described in the legend of Figure 2. The calculated pI for each spot is indicated. Molecular mass standards are indicated on the right-hand side.

phospho-acceptor site, with a consensus of L/M/I-K/R-V/S/L-x-S/T-x-x-N/E,-L/M/V/I (Figure 6A) [46]. We identified laforin-Ser[25] as a putative AMPK phosphorylation site (Figure 6B). The residues surrounding laforin Ser[25] contain four of the six consensus residues, although no basic residues are present at positions $-4/-3$ from the phospho-acceptor. In addition, Ser[25] and the surrounding residues are conserved from humans to other vertebrates and even down to protists, which also contain AMPK (Figure 6B).

To determine whether AMPK could phosphorylate laforin *in vitro*, we incubated recombinant AMPK with recombinant Hs-laforin lacking any epitope tag in the presence of [γ^{32}-P]ATP, separated the proteins by SDS/PAGE and visualized phosphorylation via autoradiography. Non-tagged laforin was phosphorylated in an AMPK-dependent manner (Figure 6C), confirming our previous results which indicated that AMPK was able to phosphorylate a GST–laforin protein fusion *in vitro* [14]. To identify the laforin residue(s) phosphorylated by AMPK, we excized bands containing laforin treated with and without AMPK from a Coomassie-Blue-stained gel, digested the proteins with trypsin and analysed the peptides by nanoLC-MS/MS. Analysis of the tryptic peptide mass spectra revealed Ser[25] and Thr[45] as the phosphorylation sites (Figure 6D and Supplementary Figure S1 at http://www.BiochemJ.org/bj/438/bj4380265add.htm). The finding that Ser[25] was a major phosphorylation site was in agreement with the data presented thus far. However, we also considered the possibility of AMPK phosphorylating laforin Thr[45] and examined the evolutionary conservation of Thr[45] and its surrounding residues. The residues around Thr[45] of Hs-laforin contain only two of the six residues of the optimal AMPK motif, and these residues, including Thr[45] itself, are not conserved in laforin even among vertebrates (Figure 6E). Since our two-hybrid data indicate that a laforin-T45A does not reduce the interaction between laforin and malin (Figure 1A) and our 2DE data indicate that Ser[25] is the major *in vivo* phosphorylation site (Figure 2A), we think that it is unlikely that Thr[45] is a physiologically relevant AMPK target and instead we think it is an *in vitro* artefact.

Next, we investigated whether AMPK phosphorylates laforin in tissue culture cells. We co-transfected HEK-293 cells with FLAG–laforin and either plasmids expressing AMPKα1 WT, AMPKα1 KD, AMPKα1 CA or an empty vector. We grew the cells to sub-confluency, replaced the medium with phosphate-free medium containing [^{32}P]P_i and MG132 (a proteasome inhibitor), incubated for 5 h and immunoprecipitated laforin using a denatured immunoprecipitation protocol [11] in order to minimize the number of non-laforin proteins that were recovered in the immunoprecipitates. We then separated the proteins by SDS/PAGE, dried the gel and exposed the gel to film. The autoradiograph demonstrates that laforin was phosphorylated in cells (Figure 6F, third lane), and this phosphorylation was enhanced by the overexpression of AMPKα1 (compare the first with the third lane). In addition, phosphorylation of laforin was improved by the overexpression of the AMPKα1 CA form (Figure 6F, fourth lane), but no effect on phosphorylation of laforin was observed when overexpressing a KD version of AMPK (Figure 6F, fifth lane).

To further prove that AMPK is involved in the *in vivo* phosphorylation of laforin, we expressed laforin in MEFs from control and double AMPKα1α2-KO mice and subjected cell extracts to 2DE. As shown in Figure 7, in MEFs from double AMPKα1α2-KO mice laforin migrated as a single spot, indicating that, in the absence of AMPK, no other protein kinases are able to phosphorylate laforin.

Cumulatively, multiple lines of evidence all confirm: (i) that AMPK is able to phosphorylate laforin both *in vitro* and *in vivo* and, (ii) that this modification occurs at residue Ser[25].

DISCUSSION

In the present paper we show evidence that laforin, a dual-specificity phosphatase involved in LD, is a phosphoprotein *in vivo* and we map the residue involved in this modification to Ser[25]. In addition, we identify AMPK as the protein kinase that phosphorylates laforin at Ser[25], both *in vitro* and *in vivo*. These results significantly extend our previous observation which suggested that AMPK phosphorylates laforin [14] by identifying the site of phosphorylation.

Laforin-Ser[25] is conserved throughout evolution. It is located in the CBD of laforin, close to the surface involved in sugar binding. We show that this residue plays critical roles in the function of laforin, since replacement of Ser[25] by alanine, a non-polar amino acid that cannot be phosphorylated, results in the loss of interaction of laforin-S25A with multiple known binding partners, such as malin, the PP1 regulatory subunit R5/PTG, and the catalytic subunit of the AMPK complex (AMPKα2). Our results also indicate that the laforin-S25A mutant exhibits decreased phosphatase activity and decreased dimerization capacity, although this change still allows binding of laforin-S25A to carbohydrates. These results may indicate that replacement of Ser[25] by an alanine residue may alter the structure of some part of the protein, resulting in loss of interaction capabilities and loss of catalytic activity. The fact that WT laforin purified from bacteria (thus unphosphorylated) has full catalytic activity, suggests again that the cause of the altered phosphatase activity observed in the laforin-S25A mutant is a conformational change and not the absence of phosphorylation. This hypothesis of laforin-S25A undergoing a structural change would explain why the resulting protein is less stable when expressed in mammalian cells. Laforin-S25A would be recognized as an aberrant protein and would be rapidly degraded by the general proteolytic system. It has been described that malin ubiquitinates laforin and targets it

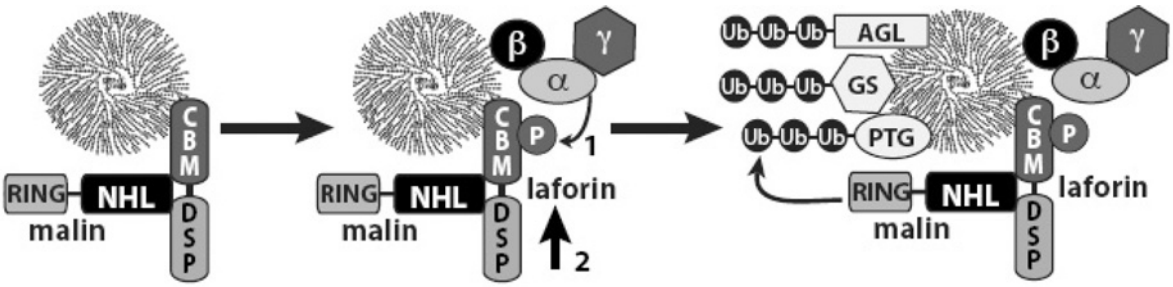

Figure 8 Proposed model of the action of the laforin–malin complex in the regulation of glycogen synthesis

The interaction between laforin and malin is enhanced by phosphorylation of laforin at Ser^{25} by AMPK (1). A more stable laforin–malin complex results (indicated by the red arrow, 2), resulting in increased ubiquitination of specific substrates, e.g. R5/PTG, glycogen synthase (GS) and AGL/GDE, leading to down-regulation of glycogen synthesis. CBM, carbohydrate-binding module; DSP, dual-specificity phosphatase; Ub, ubiquitin.

for degradation [11]. The results of the present study suggest that degradation of laforin-S25A is likely to be independent of malin, since no interaction between laforin-S25A and malin could be detected.

Some LD patients have mutations in Ser^{25}, mutating Ser^{25} to proline (S25P). Consistent with our results, a GST–laforin S25P fusion protein purified from bacteria was able to bind glycogen [47], but this laforin-S25P form did not accumulate in cell-culture systems [48]. We therefore suggest that the presence of a non-polar amino acid (either proline or alanine) at residue 25 greatly affects the functionality of the mutated laforin in terms of a loss of interaction with binding partners, decreased phosphatase activity and/or reduced protein stability due to structural changes.

In addition, we analysed the biochemical properties of laforin-S25D, mimicking a constitutive phosphorylated form. We found that this mutant is able to interact with the assayed laforin-binding partners and it is also able to dimerize. In addition, this form is able to bind to carbohydrates. However, its phosphatase activity is greatly reduced. Although speculative, these results suggest that phosphorylation of laforin may reduce its catalytic activity.

Our alanine scanning mutagenesis data identified several serine/threonine residues whose change to alanine results in an increased interaction between laforin and malin. However, since our results indicate that laforin is mainly phosphorylated on one residue (Ser^{25}), we think that the increased interaction in these other mutants is likely to be due to structural changes and not indicative of phosphorylation events.

In conclusion, in the present study we demonstrate that laforin is a phosphoprotein that is modified at residue Ser^{25} by AMPK. We have previously reported that the interaction between laforin and malin is enhanced by conditions activating AMPK [14]. Therefore we propose that phosphorylation of Ser^{25} by AMPK, although it reduces the catalytic activity of laforin, enhances the interaction of laforin with malin, improving the formation of a functional laforin–malin complex. Since both laforin and AMPK localize at the glycogen granule because they possess a CBD, phosphorylation of laforin by AMPK could recruit malin to this site (Figure 8), triggering the inactivation of glycogenic targets (i.e. R5/PTG, glycogen synthase and others) and down-regulating glycogen synthesis. If the function of the laforin–malin complex is affected (either because one of the components is not functional or because the interaction between them is prevented), no inactivation of glycogenic targets would take place, resulting in increased glycogen synthesis, which eventually would lead to the appearance of LBs.

AUTHOR CONTRIBUTION

Matthew Gentry and Pascual Sanz planned the experiments. The experiments were carried out by Carlos Romá-Mateo, Maria del Carmen Solaz-Fuster, José Vicente Gimeno-Alcañiz, Vikas Dukhande, Jordi Donderis, Alberto Marina, Olga Criado and Antonius Koller. Santiago Rodriguez De Cordoba, Matthew Gentry and Pascual Sanz analysed the data and wrote the paper.

ACKNOWLEDGEMENTS

We want to thank Dr Rafael Pulido (Centro de Investigacion Principe Felipe, Valencia, Spain) and Dr Reuben Shaw (Salk Institute, La Jolla, CA, U.S.A.) for the gift of pGEX4T1-VHR and the pEBG2-AMPK plasmids respectively. We also thank Dr Benoit Viollet (Institut Cochin, Université Paris Descartes, Paris, France) for control and AMPKα1α2-KO MEFs. We also wish to thank Miguel Heredia (CIBERER, IBV-CSIC, Valencia, Spain) and Maria Elena Fernandez-Sanchez (CIB-CSIC, Madrid, Spain) for their technical assistance in the alanine scanning mutagenesis experiments, Dr Carolyn Worby for insightful discussions, and the University of Kentucky COBRE Administrative and Proteomics Cores.

FUNDING

This work was supported the Spanish Ministry of Education and Science [grant number SAF2008-01907 (to P.S.)]; the Generalitat Valenciana [grant number Prometeo 2009/051 (to P.S.)]; the National Institutes of Health [grant numbers R00NS061803, P20RR020171, R01NS070899 (to M.S.G.)]; and the University of Kentucky College of Medicine startup funds (to M.S.G.)

REFERENCES

1 Delgado-Escueta, A. V. (2007) Advances in lafora progressive myoclonus epilepsy. Curr. Neurol. Neurosci. Rep. **7**, 428–433
2 Gentry, M. S., Dixon, J. E. and Worby, C. A. (2009) Lafora disease: insights into neurodegeneration from plant metabolism. Trends Biochem. Sci. **34**, 628–639
3 Ganesh, S., Puri, R., Singh, S., Mittal, S. and Dubey, D. (2006) Recent advances in the molecular basis of Lafora's progressive myoclonus epilepsy. J. Hum. Genet. **51**, 1–8
4 Minassian, B. A., Lee, J. R., Herbrick, J. A., Huizenga, J., Soder, S., Mungall, A. J., Dunham, I., Gardner, R., Fong, C. Y., Carpenter, S. et al. (1998) Mutations in a gene encoding a novel protein tyrosine phosphatase cause progressive myoclonus epilepsy. Nat. Genet. **20**, 171–174
5 Serratosa, J. M., Gomez-Garre, P., Gallardo, M. E., Anta, B., de Bernabe, D. B., Lindhout, D., Augustijn, P. B., Tassinari, C. A., Malafosse, R. M., Topcu, M. et al. (1999) A novel protein tyrosine phosphatase gene is mutated in progressive myoclonus epilepsy of the Lafora type (EPM2). Hum. Mol. Genet. **8**, 345–352
6 Chan, E. M., Young, E. J., Ianzano, L., Munteanu, I., Zhao, X., Christopoulos, C. C., Avanzini, G., Elia, M., Ackerley, C. A., Jovic, N. J. et al. (2003) Mutations in NHLRC1 cause progressive myoclonus epilepsy. Nat. Genet. **35**, 125–127
7 Chan, E. M., Omer, S., Ahmed, M., Bridges, L. R., Bennett, C., Scherer, S. W. and Minassian, B. A. (2004) Progressive myoclonus epilepsy with polyglucosans (Lafora disease): evidence for a third locus. Neurology **63**, 565–567

8 Minassian, B. A., Ianzano, L., Meloche, M., Andermann, E., Rouleau, G. A., Delgado-Escueta, A. V. and Scherer, S. W. (2000) Mutation spectrum and predicted function of laforin in Lafora's progressive myoclonus epilepsy. Neurology **55**, 341–346

9 Wang, J., Stuckey, J. A., Wishart, M. J. and Dixon, J. E. (2002) A unique carbohydrate binding domain targets the lafora disease phosphatase to glycogen. J. Biol. Chem. **277**, 2377–2380

10 Lohi, H., Ianzano, L., Zhao, X. C., Chan, E. M., Turnbull, J., Scherer, S. W., Ackerley, C. A. and Minassian, B. A. (2005) Novel glycogen synthase kinase 3 and ubiquitination pathways in progressive myoclonus epilepsy. Hum. Mol. Genet. **14**, 2727–2736

11 Gentry, M. S., Worby, C. A. and Dixon, J. E. (2005) Insights into Lafora disease: malin is an E3 ubiquitin ligase that ubiquitinates and promotes the degradation of laforin. Proc. Natl. Acad. Sci. U.S.A. **102**, 8501–8506

12 Lafora, G. R. and Glueck, B. (1911) Beitrag zur histogpathologie der myoklonischen epilepsie. Gesamte Neurol. Psychiatry **6**, 1–14

13 Collins, G. H., Cowden, R. R. and Nevis, A. H. (1968) Myoclonus epilepsy with Lafora bodies. An ultrastructural and cytochemical study. Arch. Pathol. **86**, 239–254

14 Solaz-Fuster, M. C., Gimeno-Alcaniz, J. V., Ros, S., Fernandez-Sanchez, M. E., Garcia-Fojeda, B., Criado Garcia, O., Vilchez, D., Dominguez, J., Garcia-Rocha, M., Sanchez-Piris, M. et al. (2008) Regulation of glycogen synthesis by the laforin-malin complex is modulated by the AMP-activated protein kinase pathway. Hum. Mol. Genet. **17**, 667–678

15 Vilchez, D., Ros, S., Cifuentes, D., Pujadas, L., Valles, J., Garcia-Fojeda, B., Criado-Garcia, O., Fernandez-Sanchez, E., Medrano-Fernandez, I., Dominguez, J. et al. (2007) Mechanism suppressing glycogen synthesis in neurons and its demise in progressive myoclonus epilepsy. Nat. Neurosci. **10**, 1407–1413

16 Cheng, A., Zhang, M., Gentry, M. S., Worby, C. A., Dixon, J. E. and Saltiel, A. R. (2007) A role for AGL ubiquitination in the glycogen storage disorders of Lafora and Cori's disease. Genes Dev. **21**, 2399–2409

17 Worby, C. A., Gentry, M. S. and Dixon, J. E. (2008) Malin decreases glycogen accumulation by promoting the degradation of protein targeting to glycogen (PTG). J. Biol. Chem. **283**, 4069–4076

18 DePaoli-Roach, A. A., Tagliabracci, V. S., Segvich, D. M., Meyer, C. M., Irimia, J. M. and Roach, P. J. (2010) Genetic depletion of the malin E3 ubiquitin ligase in mice leads to lafora bodies and the accumulation of insoluble laforin. J. Biol. Chem. **285**, 25372–25381

19 Turnbull, J., Wang, P., Girard, J. M., Ruggieri, A., Wang, T. J., Draginov, A. G., Kameka, A. P., Pencea, N., Zhao, X., Ackerley, C. A. and Minassian, B. A. (2010) Glycogen hyperphosphorylation underlies lafora body formation. Ann. Neurol. **68**, 925–933

20 Worby, C. A., Gentry, M. S. and Dixon, J. E. (2006) Laforin, a dual specificity phosphatase that dephosphorylates complex carbohydrates. J. Biol. Chem. **281**, 30412–30418

21 Tagliabracci, V. S., Turnbull, J., Wang, W., Girard, J. M., Zhao, X., Skurat, A. V., Delgado-Escueta, A. V., Minassian, B. A., Depaoli-Roach, A. A. and Roach, P. J. (2007) Laforin is a glycogen phosphatase, deficiency of which leads to elevated phosphorylation of glycogen *in vivo*. Proc. Natl. Acad. Sci. U.S.A. **104**, 19262–19266

22 Gentry, M. S., Dowen, III, R. H., Worby, C. A., Mattoo, S., Ecker, J. R. and Dixon, J. E. (2007) The phosphatase laforin crosses evolutionary boundaries and links carbohydrate metabolism to neuronal disease. J. Cell. Biol. **178**, 477–488

23 Tagliabracci, V. S., Girard, J. M., Segvich, D., Meyer, C., Turnbull, J., Zhao, X., Minassian, B. A., Depaoli-Roach, A. A. and Roach, P. J. (2008) Abnormal metabolism of glycogen phosphate as a cause for Lafora disease. J. Biol. Chem. **283**, 33816–33825

24 Ganesh, S., Agarwala, K. L., Ueda, K., Akagi, T., Shoda, K., Usui, T., Hashikawa, T., Osada, H., Delgado-Escueta, A. V. and Yamakawa, K. (2000) Laforin, defective in the progressive myoclonus epilepsy of Lafora type, is a dual-specificity phosphatase associated with polyribosomes. Hum. Mol. Genet. **9**, 2251–2261

25 Wang, W. and Roach, P. J. (2004) Glycogen and related polysaccharides inhibit the laforin dual-specificity protein phosphatase. Biochem. Biophys. Res. Commun. **325**, 726–730

26 Girard, J. M., Le, K. H. and Lederer, F. (2006) Molecular characterization of laforin, a dual-specificity protein phosphatase implicated in Lafora disease. Biochimie **88**, 1961–1971

27 Wang, Y., Liu, Y., Wu, C., Zhang, H., Zheng, X., Zheng, Z., Geiger, T. L., Nuovo, G. J., Liu, Y. and Zheng, P. (2006) Epm2a suppresses tumor growth in an immunocompromised host by inhibiting Wnt signaling. Cancer Cell **10**, 179–190

28 Liu, R., Wang, L., Chen, C., Liu, Y., Zhou, P., Wang, Y., Wang, X., Turnbull, J., Minassian, B. A., Liu, Y. and Zheng, P. (2008) Laforin negatively regulates cell cycle progression through glycogen synthase kinase 3β-dependent mechanisms. Mol. Cell. Biol. **28**, 7236–7244

29 Ito, H., Fukuda, Y., Murata, K. and Kimura, A. (1983) Transformation of intact yeast cells treated with alkali cations. J. Bacteriol. **153**, 163–168

30 Rose, M. D., Winston, F. and Hieter, P. (1990) Methods in yeast genetics, a laboratory course manual. Cold Spring Harbor Laboratory Press, Cold Spring Harbor, NY

31 Gimeno-Alcaniz, J. V. and Sanz, P. (2003) Glucose and type 2A protein phosphatase regulate the interaction between catalytic and regulatory subunits of AMP-activated protein kinase. J. Mol. Biol. **333**, 201–209

32 Shaw, R. J., Kosmatka, M., Bardeesy, N., Hurley, R. L., Witters, L. A., DePinho, R. A. and Cantley, L. C. (2004) The tumor suppressor LKB1 kinase directly activates AMP-activated kinase and regulates apoptosis in response to energy stress. Proc. Natl. Acad. Sci. U.S.A. **101**, 3329–3335

33 Ludin, K., Jiang, R. and Carlson, M. (1998) Glucose-regulated interaction of a regulatory subunit of protein phosphatase 1 with the Snf1 protein kinase in *Saccharomyces cerevisiae*. Proc. Natl. Acad. Sci. U.S.A. **95**, 6245–6250

34 Sanz, P., Alms, G. R., Haystead, T. A. and Carlson, M. (2000) Regulatory interactions between the Reg1-Glc7 protein phosphatase and the Snf1 protein kinase. Mol. Cell. Biol. **20**, 1321–1328

35 Tanner, S., Shu, H., Frank, A., Wang, L. C., Zandi, E., Mumby, M., Pevzner, P. A. and Bafna, V. (2005) InsPecT: identification of posttranslationally modified peptides from tandem mass spectra. Anal. Chem. **77**, 4626–4639

36 Soding, J., Biegert, A. and Lupas, A. N. (2005) The HHpred interactive server for protein homology detection and structure prediction. Nucleic Acids Res. **33**, W244–W248

37 Zdobnov, E. M. and Apweiler, R. (2001) InterProScan: an integration platform for the signature-recognition methods in InterPro. Bioinformatics **17**, 847–848

38 Pei, J., Tang, M. and Grishin, N. V. (2008) PROMALS3D web server for accurate multiple protein sequence and structure alignments. Nucleic Acids Res. **36**, W30–W34

39 Lambert, C., Leonard, N., De Bolle, X. and Depiereux, E. (2002) ESyPred3D: prediction of proteins 3D structures. Bioinformatics **18**, 1250–1256

40 Singh, S. and Ganesh, S. (2009) Lafora progressive myoclonus epilepsy: a meta-analysis of reported mutations in the first decade following the discovery of the EPM2A and NHLRC1 genes. Hum. Mut. **30**, 715–723

41 Machovic, M. and Janecek, S. (2006) Starch-binding domains in the post-genome era. Cell. Mol. Life Sci. **63**, 2710–2724

42 Yokota, T., Nara, Y., Kashima, A., Matsubara, K., Misawa, S., Kato, R. and Sugio, S. (2007) Crystal structure of human dual specificity phosphatase, JNK stimulatory phosphatase-1, at 1.5 Å resolution. Proteins **66**, 272–278

43 Andersen, J. N., Mortensen, O. H., Peters, G. H., Drake, P. G., Iversen, L. F., Olsen, O. H., Jansen, P. G., Andersen, H. S., Tonks, N. K. and Moller, N. P. (2001) Structural and evolutionary relationships among protein tyrosine phosphatase domains. Mol. Cell. Biol. **21**, 7117–7136

44 Hoyt, R., Zhu, W., Cerignoli, F., Alonso, A., Mustelin, T. and David, M. (2007) Cutting edge: selective tyrosine dephosphorylation of interferon-activated nuclear STAT5 by the VHR phosphatase. J. Immunol. **179**, 3402–3406

45 Liu, Y., Wang, Y., Wu, C., Liu, Y. and Zheng, P. (2006) Dimerization of laforin is required for its optimal phosphatase activity, regulation of GSK3β phosphorylation, and Wnt signaling. J. Biol. Chem. **281**, 34768–34774

46 Gwinn, D. M., Shackelford, D. B., Egan, D. F., Mihaylova, M. M., Mery, A., Vasquez, D. S., Turk, B. E. and Shaw, R. J. (2008) AMPK phosphorylation of raptor mediates a metabolic checkpoint. Mol. Cell **30**, 214–226

47 Ganesh, S., Tsurutani, N., Suzuki, T., Hoshii, Y., Ishihara, T., Delgado-Escueta, A. V. and Yamakawa, K. (2004) The carbohydrate-binding domain of Lafora disease protein targets Lafora polyglucosan bodies. Biochem. Biophys. Res. Commun. **313**, 1101–1109

48 Ganesh, S., Delgado-Escueta, A. V., Suzuki, T., Francheschetti, S., Riggio, C., Avanzini, G., Rabinowicz, A., Bohlega, S., Bailey, J., Alonso, M. E. et al. (2002) Genotype-phenotype correlations for EPM2A mutations in Lafora's progressive myoclonus epilepsy: exon 1 mutations associate with an early-onset cognitive deficit subphenotype. Hum. Mol. Genet. **11**, 1263–1271

Received 24 January 2011/27 May 2011; accepted 28 June 2011
Published as BJ Immediate Publication 28 June 2011, doi:10.1042/BJ20110150

Biochem. J. (2011) **439**, 265–275 (Printed in Great Britain) doi:10.1042/BJ20110150

online data

SUPPLEMENTARY ONLINE DATA

Laforin, a dual-specificity phosphatase involved in Lafora disease, is phosphorylated at Ser[25] by AMP-activated protein kinase

Carlos ROMÁ-MATEO*, Maria del Carmen SOLAZ-FUSTER*, José Vicente GIMENO-ALCAÑIZ*, Vikas V. DUKHANDE†, Jordi DONDERIS*, Carolyn A. WORBY‡, Alberto MARINA*, Olga CRIADO§, Antonius KOLLER‖, Santiago RODRIGUEZ DE CORDOBA§, Matthew S. GENTRY†[1,2] and Pascual SANZ*[1,2]

*Instituto de Biomedicina de Valencia, CSIC and Centro de Investigación Biomédica en Red de Enfermedades Raras (CIBERER), Jaime Roig 11, 46010 Valencia, Spain, †Department of Molecular and Cellular Biochemistry and Center for Structural Biology, University of Kentucky, Lexington, KY 40536-0509, U.S.A., ‡Departments of Pharmacology, Cellular and Molecular Medicine, and Chemistry and Biochemistry, University of California San Diego, La Jolla, CA 92093-0721, U.S.A., §Centro de Investigaciones Biológicas, CSIC and Centro de Investigación Biomédica en Red de Enfermedades Raras (CIBERER), Ramiro de Maeztu 9, 28040 Madrid, Spain, and ‖Proteomics Center, SUNY-Stony Brook, School of Medicine, Stony Brook, NY 11794-8691, U.S.A.

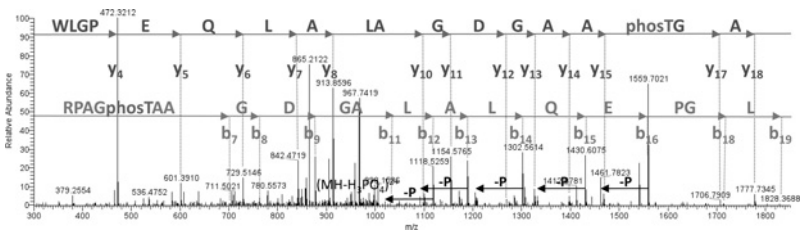

Figure S1 AMPK phosphorylates laforin at Thr[45] *in vitro*

Non-tagged recombinant laforin was incubated in kinase buffer (see the Experimental section of the main text) in the presence or absence of AMPK, as described in Figure 5 of the main text. Reactions were quenched, proteins separated by SDS/PAGE, the gel was stained with Coomasie Blue, and bands corresponding to non-phosphorylated and phosphorylated laforin were excized and analysed by MS.

Received 24 January 2011/27 May 2011; accepted 28 June 2011
Published as BJ Immediate Publication 28 June 2011, doi:10.1042/BJ20110150

[1] These senior authors contributed equally to this work.
[2] Correspondence may be addressed to either of these authors (email matthew.gentry@uky.edu or sanz@ibv.csic.es).